

## RESEARCH ARTICLE

# Behavioral and mechanical determinants of collective subsurface nest excavation

Daria Monaenkova, Nick Gravish, Gregory Rodriguez, Rachel Kutner, Michael A. D. Goodisman and Daniel I. Goldman\*

## ABSTRACT

Collective construction of topologically complex structures is one of the triumphs of social behavior. For example, many ant species construct underground nests composed of networks of tunnels and chambers. Excavation by these ‘superorganisms’ depends on the biomechanics of substrate manipulation, the interaction of individuals, and media stability and cohesiveness. To discover principles of robust social excavation, we used X-ray computed tomography to monitor the growth in three dimensions of nests built by groups of fire ants (*Solenopsis invicta*) in laboratory substrates composed of silica particles, manipulating two substrate properties: particle size and gravimetric moisture content. Ants were capable of nest construction in all substrates tested other than completely dry or fully saturated; for a given particle size, nest volume was relatively insensitive to moisture content. Tunnels were deepest at intermediate moisture content and the maximum tunnel depth correlated with measured yield force on small rod-shaped intruders (a proxy for cohesive strength). This implies that increased cohesive strength allowed creation of tunnels that were resistant to perturbation but did not decrease individual excavation ability. Ants used two distinct behaviors to create pellets composed of wetted particles, depending on substrate composition. However, despite the ability to create larger stable pellets in more cohesive substrates, pellet sizes were similar across all conditions. We posit that this pellet size balances the individual’s load-carrying ability with the need to carry this pellet through confined crowded tunnels. We conclude that effective excavation of similarly shaped nests can occur in a diversity of substrates through sophisticated digging behaviors by individuals which accommodate both differing substrate properties and the need to work within the collective.

**KEY WORDS:** *Solenopsis invicta*, Fire ants, Nest construction, Soil cohesion, X-ray

## INTRODUCTION

Approximately 85% of soil-dwelling fauna is composed of digging and burrowing arthropods (Decaëns et al., 2006). Subterranean life in complex materials like soil and sand has substantial advantages. For example, animals that live underground avoid high temperatures, low humidity and predation (Tschinkel, 2006). Previous research on subterranean animals has revealed that digging behaviors of arthropods are remarkably versatile and sophisticated (Evans, 1966; Muma, 1967; Rutin, 1996; Price and May, 2009; Springthorpe et al., 2013), allowing individual organisms to create

structures in a diversity of substrates. However, less is known about how collectives of social animals work together to excavate complex materials.

Highly social animals, such as social insects, form colonies that are sometimes referred to as ‘superorganisms’ because of the remarkable integration of behaviors that help the collective survive and reproduce (Hölldobler and Wilson, 2009). For example, many termites and ants create subterranean nests in soil, which allows colonies to perform functions such as protection (Huang, 2010) and processing of food (Mason, 1958), rearing young (Kadochova and Frouz, 2013) and thermoregulation (Korb, 2003). Superorganism nests are marvels of complexity, consisting of interconnected tunnels and chambers. The topology of the nest networks is primarily a function of the collective behavior of the society (Buhl et al., 2004a,b; Lee et al., 2007; Bardunias and Su, 2010).

Both individual and superorganismal excavators face challenges in the manipulation and handling of deformable and breakable pellets (Ratcliffe and Fagerstrom, 1980; Villani et al., 1999; Strauch and Herminghaus, 2012). For instance, soil moisture content plays important roles in excavation (Ali et al., 1986; Tschinkel, 2006). The moisture content of the soil can influence activity rates of subterranean animals (Rhoades and Davis, 1967; Whitford and Ettershank, 1975; Coleman et al., 2004; Sprague, 2013; Pielström and Roces, 2014), the integrity of transported material (Espinoza and Santamarina, 2010), the stability of structures (Aleksiev et al., 2007), the intensity of excavation (Espinoza and Santamarina, 2010; Toffin et al., 2010; Minter et al., 2013) and desiccation costs (Coleman et al., 2004; Sprague, 2013). Particle size also plays an important role in nest construction, affecting the strategy used to transport material, transfer speed (Burd, 2000) and nest design (Farji-Brener, 2003).

Such materials challenge physical scientists as well; the response of wet granular media subject to external loads is an active area of research (Campbell et al., 1980; Nowak et al., 2005; Strauch and Herminghaus, 2012; Mitarai and Nori, 2006). In wet sandy soils, water forms liquid bridges among particles, which act to attract neighboring particles, increasing cohesiveness of the substrates. This is important because the relative strength of cohesive forces to particle weight plays an important role in the stability of agglomerates of wet granular media and structures composed of these materials. But little is known about wet granular media in situations relevant to animal excavation.

Superorganismal excavators are presented with additional complexity aside from the need to pull apart, form and transport complex materials. Specifically, they must perform their substrate manipulations in the presence of thousands of neighbors and move soil thousands of body lengths through complex networks. These circumstances can lead to tradeoffs. For example, an individual could choose to maximize the size of a pellet to maximize the amount of soil transported per trip from the tunnel face to the

School of Physics, Georgia Institute of Technology, 837 State Street NW, Atlanta, GA 30332-0430, USA.

\*Author for correspondence (daniel.goldman@physics.gatech.edu)

Received 11 September 2014; Accepted 27 February 2015

**List of symbols and abbreviations**

$A_p$	pellet size
$\bar{A}_p$	mean pellet size
CT	computed tomography
$D$	nest depth
$d$	substrate particle diameter
$F_y$	yield force
$E$	number of network edges
$F_d$	drag force
$h$	animal head size
$k$	vertex degree
$l$	edge length
$V$	nest volume
$V_p$	pellet volume
$W$	substrate moisture
$\Delta V/\Delta t$	volumetric growth rate of the nest
$v$	number of network vertices

surface (in accord with optimal foraging theory; Hooper-Bùi et al., 2002). In this scenario, load size during excavation would be limited by the size and the strength of the individual ant, as well as soil properties like cohesiveness, particle size and particle shape. However, such a strategy might be counter-productive as individuals carry pellets over thousands of body lengths, within dark, narrow and crowded environments filled with other ants moving at multiple body lengths per second (Gravish et al., 2013) (Fig. 1A). Thus, large pellets could break via perturbations from the environment and other ants, or lead to traffic jams and tunnel clogs. An alternative strategy would be for individuals to transport small pellets, which would not interfere with the activities of colony mates. Such transport, though, might be inefficient, requiring many trips to and from the tunnel face. Therefore, because of these competing scenarios, the social aspects of collective excavation (Sakagami and Hayashida, 1962; Sudd,

1972) and abilities of the individuals might not be predictive of the performance for the collective.

The red imported fire ant (*Solenopsis invicta* Buren 1972, Fig. 1A) represents an excellent example of a successful collective excavator. Colonies of fire ants may contain hundreds of thousands of ~3.5 mm long workers and construct nests over a meter deep (Tschinkel, 2006), with tens of meters of horizontal tunnels radiating away from the nest for foraging. Such structures are initially built quickly (allowing the bulk of the colony to move below ground) and can last many years (Markin et al., 1973). Fire ant nests are built by individuals through the formation and transport of ‘pellets’, agglomerates of soil. Fire ants are adept at excavating (forming) pellets in sandy soil with particles comparable in size to their head size, as well as clay-like substrates, which contain particles tens of times smaller and form a nearly continuous medium (Taber, 2000; Tschinkel, 2006). In the roughly 80 years since their arrival in North America, fire ants have colonized over 300 million acres (Oi et al., 2008) in the US alone, creating nests in diverse environmental and soil conditions.

In this study, we sought to discover how social animals excavate so effectively and thereby to discover principles at the macroscale (nest level) and microscale (individual level) by which superorganisms collectively excavate nests. We used fire ants as a model system for studying collective nest excavation. We employed a new technique to create a variety of representative substrates using particle size and moisture content to control both the cohesiveness of the substrates and the challenges faced by the ants (e.g. wet large particles with low cohesion, small particles with high cohesion, etc.). We then used X-ray computed tomography (CT) to resolve three-dimensional (3D) incipient nest (tunnel) morphology and evolution in space and time. We connected observed nest features to cohesive properties of the substrates by performing granular penetration and drag experiments. We then connected the macroscale measurements of the nest to microscale efforts of the individuals through the use of video imaging to monitor the excavation behaviors and to examine the size of loads carried as ants dig at the advancing tunnel face. Our studies of the macroscale and microscale manipulation lead to a hypothesis of optimal pellet size, which balances individual carrying capacity against clogging, pellet disruption, locomotor hindrance and other issues associated with operating in a collective, crowded environment. Our experiments also begin to reveal the diversity of mechanisms by which collectives of social animals successfully excavate subterranean environments.

**RESULTS****Physical aspects of the nest in varying substrate conditions****Substrate creation and variables measured**

We challenged groups of  $100 \pm 10$  *S. invicta* workers to construct nests in model substrates. Because natural soils can be heterogeneous – composed of different sized particles and different amounts of water – we chose to simplify the substrates by creating homogeneous wet media with particles of different diameters  $d$ . We will refer to preparations such as ‘clay-like’ ( $d=0.025 \pm 0.025$  mm), ‘fine’ sand-like ( $d=0.24 \pm 0.03$  mm) and ‘coarse’ sand-like ( $d=0.7 \pm 0.1$  mm) substrates (Fig. 1B) throughout the paper.

We used a newly developed apparatus described in Materials and methods to control the compaction and gravimetric moisture content ( $W$ , defined as the ratio of total water weight to total solid weight) within each substrate. We performed experiments in dry and unsaturated substrates with  $W=0.0, 0.01, 0.03, 0.05, 0.1, 0.15, 0.18, 0.2$  and fully saturated substrates with  $W$  ranging between 0.22 and 0.28 depending on particle size. (Fig. 2A).

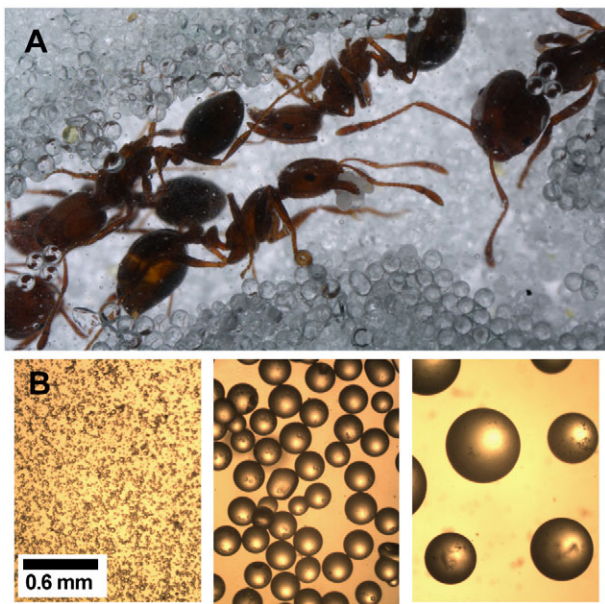


**Fig. 1. Fire ant excavation and laboratory models of different soil types.** (A) Fire ants construct subterranean tunnels through the removal of soil. In this image, fire ants remove wetted glass particles by carrying them in their mandibles. (B) Samples of laboratory substrates (left to right): clay-like (particle diameter  $d=0.025 \pm 0.025$  mm), fine sand-like ( $d=0.24 \pm 0.03$  mm) and coarse sand-like ( $d=0.7 \pm 0.1$  mm).

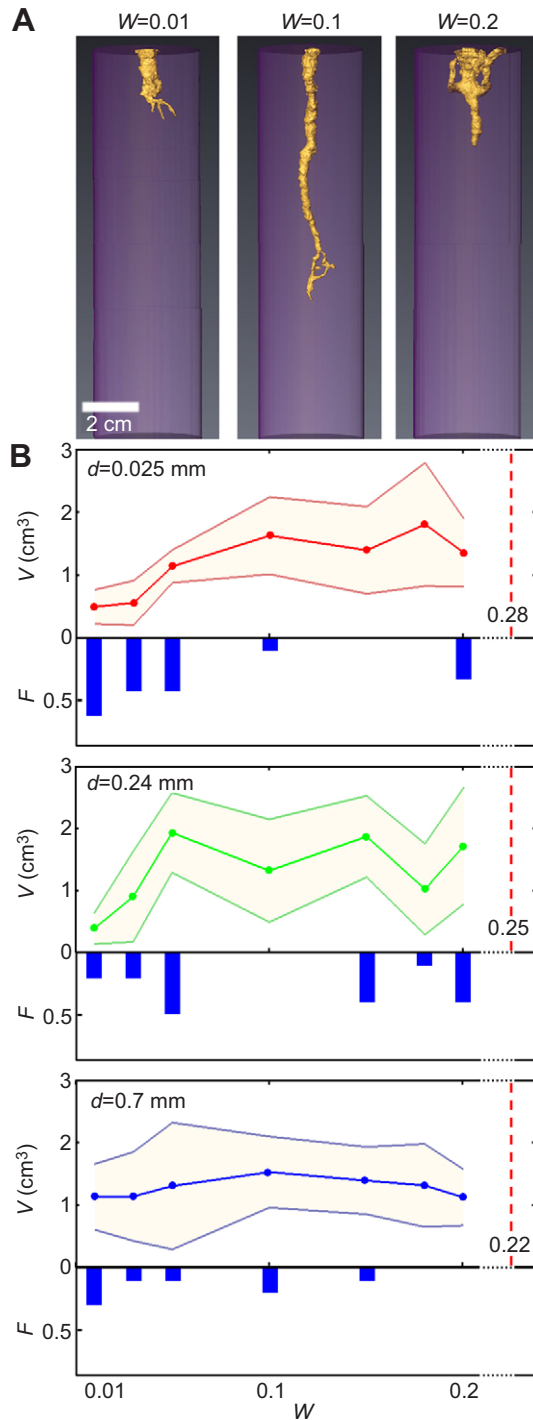


**Fig. 2. Nest volume variation with substrate moisture.** (A) 3D reconstructions of nests built by groups of fire ants in the  $d=0.7$  mm substrate (coarse) at moisture contents  $W=0.01$ , 0.1 and 0.2. (B) Upper graphs show the effect of substrate moisture,  $W$ , on the volume,  $V$ , of nests constructed within 20 h in substrates of different sizes,  $d$  (means $\pm$ s.d.). Lower graphs show the fraction  $F$  of experiments in which a nest was not constructed. Dashed red lines indicate empirically determined  $W$ , corresponding to full substrate saturation.

Properties of 3D tunnels constructed by the ants, such as depth ( $D$ ), volume ( $V$ ), volumetric growth rate ( $\Delta V/\Delta t$ ) and topological traits of the nest network, were obtained using a custom-made X-ray CT system described in Materials and methods. The depth of the nest was defined as the maximum vertical distance

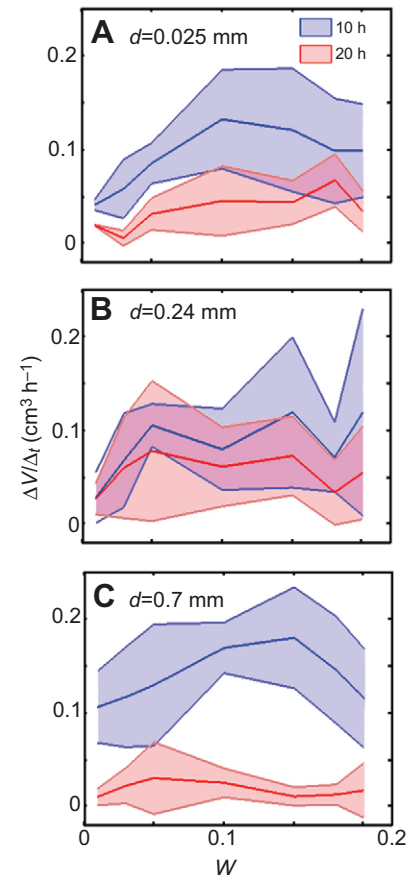


**Fig. 3. Variation of substrate excavation rates as a function of substrate moisture after 10 and 20 h of nest construction.** Variation of volumetric excavation rates,  $\Delta V/\Delta t$ , with substrate moisture,  $W$ , in substrates of different particle sizes,  $d$ , after 10 h (the first epoch) and 20 h (the second epoch) of excavation: (A) clay-like, (B) fine and (C) coarse. Shaded regions show s.d.

reached by the ants from the substrate surface (Fig. 4C) within 20 h.

#### Excavated volume and nest growth rate for varying particle size and moisture

As a measure of excavation efficacy, we first analyzed the total volume excavated in 20 h (Fig. 2). In some conditions, the ants reached the bottom of the container within the 20 h period. Fire ants were capable of nest construction in all conditions, with the exception of completely dry ( $W=0$ ) and fully saturated substrates ( $W=0.22$  for coarse,  $W=0.25$  for fine and  $W=0.28$  for clay-like substrates). As demonstrated below, the biomechanical strategy of substrate manipulation was influenced by the particle size. Because of this, the effect of moisture content on nest excavation efficacy was tested for each particle size separately. Linear regression revealed a statistically significant correlation between nest volume and moisture content in clay-like ( $R^2=0.191$ ,  $N=45$ ,  $P=0.0027$ ) and fine ( $R^2=0.104$ ,  $N=45$ ,  $P=0.031$ ) substrates. Linear regression also demonstrated that the volume of the nests built in these substrates was insensitive to moisture content at moderate  $W$  ( $0.05 < W \leq 0.2$ ) and decreased significantly at  $W \leq 0.03$  (Fig. 2B). In coarse substrates, the effect of  $W$  on  $V$  was not significant ( $R^2=0.001$ ,  $N=56$ ,  $P=0.82$ ). Multiway regression of nest volume on particle size and moisture content revealed that at low substrate moistures ( $W \leq 0.03$ ) the volume of the nest significantly increased with increasing particle size ( $R^2=0.23$ ,  $P=0.0072$ ,  $N=36$ ). At moderate

moistures ( $0.05 < W \leq 0.2$ ) the effect of particle size was not significant. We note that in almost all substrate conditions there was a fraction of trials ( $F$ ) for which the ants did not dig in 20 h (Fig. 2B).

Our imaging system allowed measurement of the development of the nest over time. The volumetric growth rates of the nest were compared after 10 and 20 h of the experiment (which for convenience we denote as ‘epochs’). A multiple regression model against particle size ( $R^2=0.54$ ,  $P=0.003$ ,  $N=294$ ),  $W$  ( $R^2=0.54$ ,  $P=0.0021$ ,  $N=294$ ) and epoch ( $R^2=0.54$ ,  $P<0.0001$ ,  $N=294$ ) predicted the statistically significant contribution of all factors to the nest excavation rates. Overall, the nest growth rate increased with substrate coarseness. The highest excavation rate occurred within the first epoch in fine substrates (up to  $0.3 \text{ cm}^3 \text{ h}^{-1}$ ). A multiple regression of volumetric growth rate  $\Delta V/\Delta t$  on epoch and moisture content performed in every substrate separately revealed that both variables significantly affected  $\Delta V/\Delta t$  in clay-like ( $R^2=0.55$ , time:  $P<0.0001$ ,  $W$ :  $P=0.0094$ ,  $N=90$ ) and fine ( $R^2=0.31$ , time:  $P<0.0001$ ,  $W$ :  $P=0.042$ ,  $N=90$ ) substrates. In these substrates, the growth rates decreased with epoch and increased with  $W$  (Fig. 3A,B). For experiments in coarse substrates,  $\Delta V/\Delta t$  was significantly affected by epoch ( $R^2=0.73$ ,  $P<0.0001$ ,  $N=114$ ), but not moisture content (Fig. 3C).

#### Nest tunnel depth and branching

We next investigated geometrical aspects of the excavated nests: the tunnel depth,  $D$ , and the amount of tunnel branching, defined as the ratio of the total tunnel length to the length of the longest tunnel of the network (Fig. 4). Our previous studies demonstrated that tunnel diameter was insensitive to substrate properties for a range of substrate conditions (Gravish et al., 2013). As in our measurements of nest volume, we used linear regression analysis to assess the effect of moisture content on maximum tunnel depth in each substrate separately (Fig. 4A). This analysis revealed a statistically significant relationship between tunnel depth and moisture content in clay-like ( $R^2=0.207$ ,  $P=0.0017$ ,  $N=45$ ) and fine ( $R^2=0.25$ ,  $P=0.0005$ ,  $N=45$ ) substrates, but an absence of a relationship in coarse substrates ( $R^2=0.015$ ,  $P=0.367$ ,  $N=56$ ). In all substrates, the shortest tunnels were constructed at low moisture contents where, depending on particle size, tunnel depth was 2–3 times lower than the maximum depth reached by the ants in the same substrate (supplementary material Table S1). Also, linear regression indicated a significant increase in tunnel branching with increasing moisture content in coarse substrates ( $R^2=0.297$ ,  $P<0.0001$ ,  $N=57$ ), and a weaker, but still significant, positive effect of  $W$  on branching in clay-like ( $R^2=0.123$ ,  $P=0.0182$ ,  $N=45$ ) and fine substrates ( $R^2=0.16$ ,  $P=0.0065$ ,  $N=45$ ) (Fig. 4B). On average, the highest branching was observed in wet ( $W=0.2$ ) coarse substrates (Fig. 4B), and in these substrates the linear correlation of average tunnel depth and average nest volume was weaker ( $R^2=0.71$ ,  $P=0.018$ ,  $N=7$ ) in comparison to clay-like ( $R^2=0.96$ ,  $P=0.0001$ ,  $N=7$ ) and fine ( $R^2=0.93$ ,  $P=0.0005$ ,  $N=7$ ) substrates (Fig. 5A).

#### The relationship between nest properties and substrate cohesiveness

We measured the effects of substrate cohesiveness on nest volume. We focused our study on the ‘granular’ – the coarse and fine particles with  $d$  greater than approximately  $100 \mu\text{m}$  – substrates in which interparticle attractive forces (like van der Waals and electrostatic) in such particles are small compared with particle weight (Espinoza and Santamarina, 2010). In substrates with  $d < 100 \mu\text{m}$ , like the clay-like particles, interparticle attraction through non-water-based forces can be important. Thus, using the granular particles with varying moisture content allowed for systematic and controlled variation of cohesiveness.

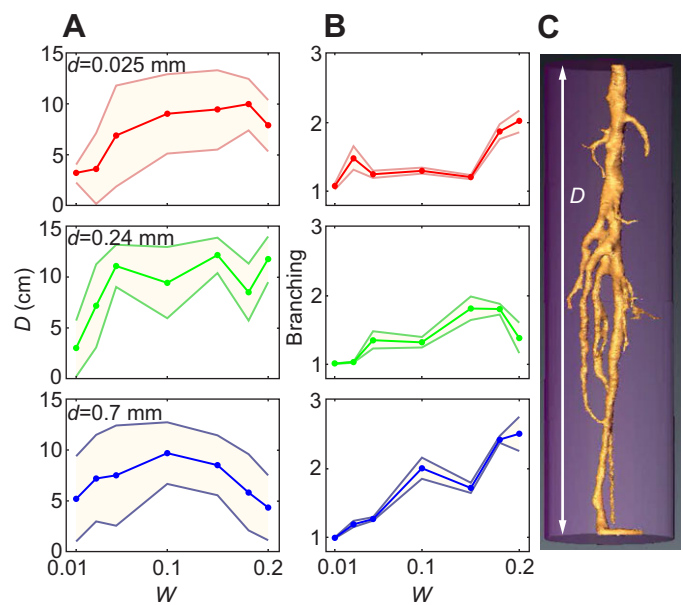


**Fig. 4. Depth and network branching of nests constructed in different substrates.** The dependence of (A) nest depth,  $D$ , and (B) tunnel branching on substrate moisture,  $W$ . Results are ordered vertically by substrate particle size,  $d$ . All data are means  $\pm$  s.d. (C) A 3D reconstruction from X-ray CT of a nest with high branching number constructed at  $W=0.18$ .

We characterized cohesiveness as the peak force required to make the substrate flow upon a localized disturbance: the substrate localized yield force,  $F_y$ , the measurement of which is described in Materials and methods. In fine substrates,  $F_y$  increased with increasing moisture content. In coarse substrates,  $F_y$  initially increased with increasing  $W$ , but then decreased for  $W > 0.15$  (Fig. 5B). The lowest  $F_y$  was measured in completely dry and wet substrates, where the ants did not excavate the nest.

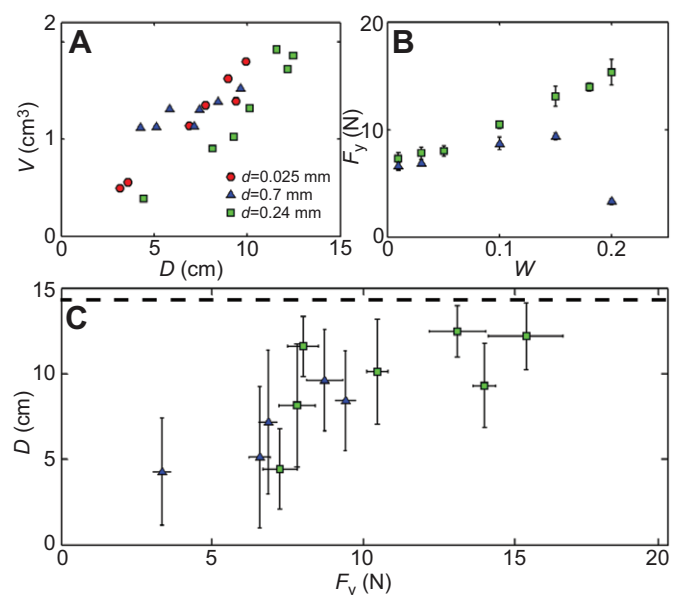


**Fig. 5. The correlation of nest depth with substrate yield force.** (A) Average values of nest volumes,  $V$ , plotted versus average values of nest depths,  $D$ , for each particle size. Averages were computed for trials at a given substrate moisture content,  $W$ ; see supplementary material Table S1 for s.d. (B) Effect of  $W$  on the yield force,  $F_y$ . (C) Depth,  $D$ , is correlated with  $F_y$  in fine and coarse substrates. Error bars show s.d. Dashed line indicates container depth.

In principle, large  $F_y$  could favor the construction of either small nests through an inability to remove pellets or large nests through increased stability of excavated structures. Our comparison of the physical and biological measurements revealed the latter (Fig. 5C). Linear regression showed a positive correlation between tunnel depth and yield force in fine ( $R^2=0.26$ ,  $P=0.0002$ ,  $N=47$ ) and coarse ( $R^2=0.25$ ,  $P=0.0012$ ,  $N=39$ ) particles (Fig. 5C). At intermediate yield force, depth was most sensitive to  $F_y$ . At low  $F_y$ , ants dug minimally, and at high  $F_y$ , excavation depth was insensitive to  $F_y$  and was limited by the depth of the digging arena.

### Network properties in 3D and comparison with quasi-2D systems

To investigate topological (network) features of the 3D reconstructions of the nests (Fig. 4C), we utilized methods from graph theory that have been successfully applied for description of animal nests built in both 2D (Buhl et al., 2004a, b) and 3D (Perna et al., 2008). In this approach, the nest is viewed as a network of tunnels in which the tunnels are the edges of the network and the vertices are the branching or end points of the tunnels (Fig. 6A). The following network features were quantified and compared for the nests built in different substrate types: the number of edges,  $E$ , and edge length,  $l$ , the number of vertices,  $v$ , and vertex degree,  $k$  (the number of edges emanating from a vertex). The vertex degree is the measurement of tunnel branching; a degree higher than one suggests that more than one tunnel emanated from the vertex.

Two-way chi-square analysis revealed significant effects of particle size  $d$  ( $\chi^2=13.069$ ,  $P=0.0003$ ,  $N=1085$ ) and  $W$  ( $\chi^2=41.844$ ,  $P<0.0001$ ,  $N=1085$ ) on the vertex degree. The probability that the network featured simple tunnels with 1 degree vertices decreased with an increase in moisture content and an increase in substrate coarseness. The effect of the interaction term of particle size and moisture content was not significant.

We compared the properties of networks built in the fine substrates with our previous topological measurements of networks built in quasi-2D setups (Gravish et al., 2012) in substrates of comparable  $d$  (Fig. 6B–D). In both 2D ( $R^2=0.989$ ,  $P<0.0001$ ,  $N=116$ ) and 3D ( $R^2=0.976$ ,  $P<0.0001$ ,  $N=42$ ) settings, the number of edges linearly increased with the number of vertices, with the slope slightly higher than unity, which indicates branched networks containing a small number of closed loops (or tunnels connecting vertical network branches) (Fig. 6C). A one-way ANOVA test of the proportion of 1 and 3 degree vertices in the experiment showed no significant difference between quasi-2D and 3D settings. In both cases, networks featured a large fraction of 1 degree ( $\sim 0.7$ ) and 3 degree ( $\sim 0.3$ ) vertices (Fig. 6B).

The probability distribution of the edge length in 2D and 3D cases was consistent with a power law  $P(l)=Q(l+l_0)^\delta$  previously used by Gravish et al. (2012) (Fig. 6D). The coefficient  $Q$  was constrained, as  $\int_0^\infty P(l)dl=1$  and  $\delta=-1.9$  and  $l_0=0.7$  (non-linear regression,  $R^2=0.91$ ,  $P<0.0001$ ) for 3D networks and  $\delta=-1.8$  and  $l_0=1.5$  (non-linear regression,  $R^2=0.71$ ,  $P<0.0001$ ) for 2D networks. Finally, we note that the excavation rates within 12 h in 3D containers enclosing 100 ants varied between  $\sim 0.05$  and  $0.3 \text{ cm}^3 \text{ h}^{-1}$ , while in 2D settings (Gravish et al., 2012) in experiments with  $\sim 150$  ants the rates were slightly higher at  $\sim 0.4 \text{ cm}^3 \text{ h}^{-1}$ . The diameters of constructed tunnels were independent of substrate conditions and comparable to ant size: 3–5 mm in both experimental settings.

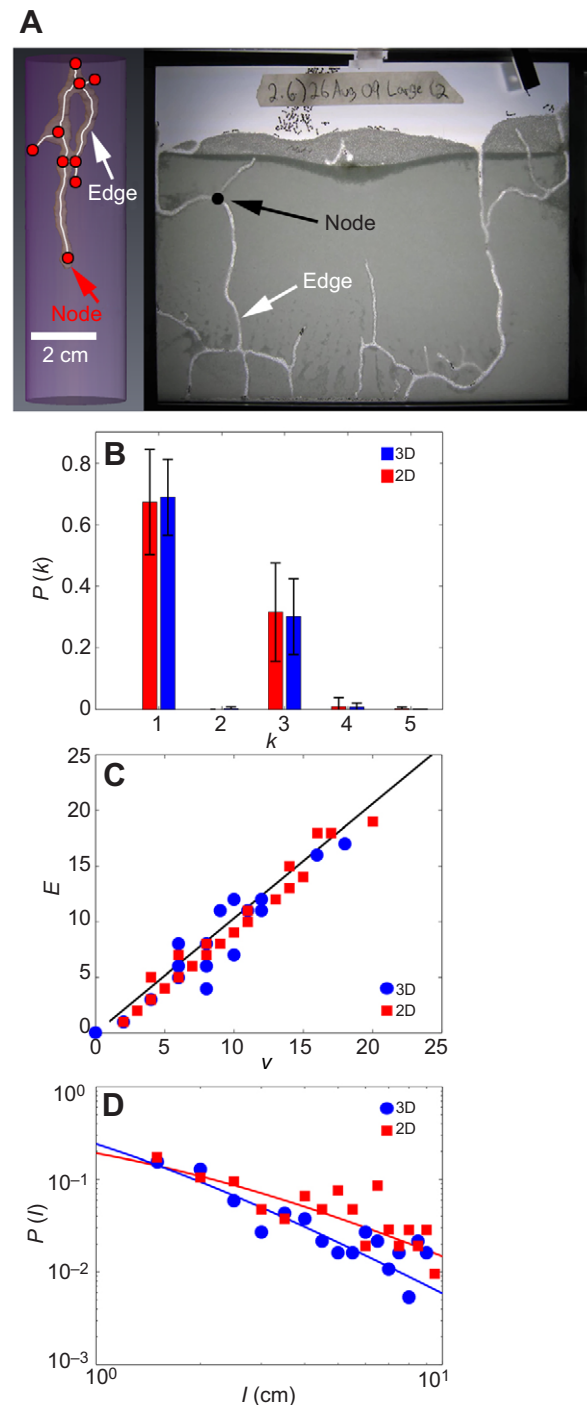


**Fig. 6. Comparison of morphological traits of 3D and 2D nests in fine substrates.** (A) Example of 3D and 2D networks. (B) Probability of vertex degree ( $k$ ) distribution in networks built in 2D and 3D experiments (error bars show s.d.). (C) Relationship between the number of edges ( $E$ ) and number of vertices ( $v$ ) for networks built in 2D and 3D setups after 20 h of excavation. (D) Probability of edge length ( $l$ ) distributions in 2D and 3D networks after 20 h. Data for 2D networks are taken from previous work (Gravish et al., 2012). Data for vertex degree, vertex–edge relationship and edge–length distribution are shown for fine substrates over all water contents.

### Excavation behaviors under changing substrate conditions

We conducted excavation experiments in quasi-2D settings to understand how individual ant-digging behaviors differed in different substrates. Groups of 30 ants were induced to dig in a

cylindrical container near a transparent sidewall (Materials and methods) and subsurface behaviors of individual ants were monitored. Groups consisted of both small and large ants selected according to their head size,  $h$  (Materials and methods). The experiments were conducted in substrates of different particle sizes, each at  $W=0.01$  and  $W=0.1$ .

Fire ants excavated substrate using two distinct behaviors, each consisting of a series of stereotypical movements of mouthparts, appendages and antennae. In the ‘pulling’ mode, an ant grasped a pellet (or a single particle in coarse substrates) and pulled it away from the tunnel wall (Fig. 7A; supplementary material Movie 1). Successful pellet extraction was followed by transport to the tunnel exit. Ants were capable of the manipulation of particles that could not fit in their mandibles. In these cases, the ant grasped the particle between the head and the forelimbs, and then used the midlimbs and hindlimbs for locomotion.

The ‘formation’ mode involved the active creation of a pellet. In this case, substrate loosening was assisted by raking the mandibles and forelimbs against the tunnel surface. The loosened substrate was then collected under the thorax (Fig. 7B; supplementary material Movie 2). The ant (with its head oriented downward) was supported by the midlimbs and hindlimbs anchored at the tunnel walls. After three to seven approaches, the accumulated substrate was compressed between the animal’s thorax, mandibles, forelimbs and midlimbs to create a pellet (Fig. 7B). The ant transported the pellet from the digging site in its mandibles. The formation mode was supported by use of the antennae as sensory organs to probe the surface of the tunnel during substrate compaction and to adjust the pellet position in the mandibles during transport. Similar behavior was observed in natural substrates (moist Georgia sand and clay) in a separate set of control experiments.

We expected that the dominant mode of excavation would be affected by particle size, moisture content and animal head size. A three-way chi-square test demonstrated that the frequency of excavation behaviors was significantly affected by  $d$  ( $\chi^2=118.45$ ,  $P<0.0001$ ,  $N=629$ ) and the interaction of particle size and moisture content ( $\chi^2=4.44$ ,  $P=0.035$ ,  $N=629$ ). The pulling mode

was the dominant excavation behavior in coarse substrates while the formation mode was used in clay-like and fine substrates. Moisture content, head size alone, or other interaction terms of the model had no significant effect on the frequency of excavation behaviors.

Both excavation modes incorporated coordinated movements of the head, mandibles, limbs and, surprisingly, the antennae. The active use of antennae in the excavation, manipulation is interesting, given that the role of antennae has been thought to be largely sensory (Tschinkel, 2006). Further, during pellet transport, antennae were used to adjust pellet position in the mouthpart. These observations complement our recent discovery of antennae usage for stabilization during confined locomotion (Gravish et al., 2013).

We also expected that ants would create larger pellets in more cohesive substrates. Indeed, mean pellet size,  $\bar{A}_p$ , was smaller in lower moisture content substrates, as pellet cohesiveness increases with increasing moisture content; however, the effect was weak (supplementary material Table S2). In fact, the increase in the mean size  $\bar{A}_p$  of the pellets in these substrates did not exceed 20%. Three-way ANOVA demonstrated that within this variation in the size of pellets,  $A_p$  (see Materials and methods), there were significant effects on  $A_p$  of particle size ( $F_{2,1891}=10.466$ ,  $P<0.0001$ ), moisture content ( $F_{1,1891}=12.014$ ,  $P=0.0005$ ), head size ( $F_{1,1891}=55.375$ ,  $P<0.0001$ ), the two-way interaction between particle and head size ( $F_{2,1891}=28.511$ ,  $P<0.0001$ ), and the three-way interaction between all factors ( $F_{2,1891}=5.394$ ,  $P=0.0046$ ). One-way ANOVA was applied to test the effect of  $h$  on  $A_p$  in each substrate separately. In the coarse substrates, there was no effect of  $h$  on  $A_p$ , which was close to the size of a single particle. In clay-like ( $F_{1,872}=9.221$ ,  $P<0.0025$ ) and fine ( $F_{1,592}=134.55$ ,  $P<0.0001$ ) substrates, where the formation mode dominated,  $A_p$  was positively correlated with head size (supplementary material Table S2). The small variations of pellet size with moisture content, particle size and head width are interesting given that ants could clearly create larger pellets (e.g. some pellets were up to 7 times larger than the mean pellet size; Fig. 8; supplementary material Table S2). We expect that the significant increase in nest volumes and nest excavation rates with increasing  $W$  can be attributed not only to the larger pellet sizes but also to the rise in excavation activity of ants. The latter is a result of either a larger number of workers participating in excavation or a higher frequency of runs performed by individual workers.

## DISCUSSION

We challenged groups of fire ants to create nests within substrates composed of controlled preparations of granular media and water to understand the mechanics of collective nest-building behavior. At the ‘macroscale’, 3D X-ray CT reconstructions of the time evolution of incipient nests revealed that nest volumes after 20 h were insensitive to substrate type (varying particle size and moisture content) once moisture content was sufficiently high. At the ‘microscale’, visible light imaging of individual ant behaviors at the faces of the tunnels revealed that fire ants used sophisticated manipulation strategies to create similar sized pellets in all tested materials. We now discuss both our macroscale and microscale results, and show how they indicate that constraints on digging and transport (and thus the emergent structure of the nest) are determined by the cohesiveness of the substrate, the ability of an individual to manipulate granular substrate and the need to operate within a collective.

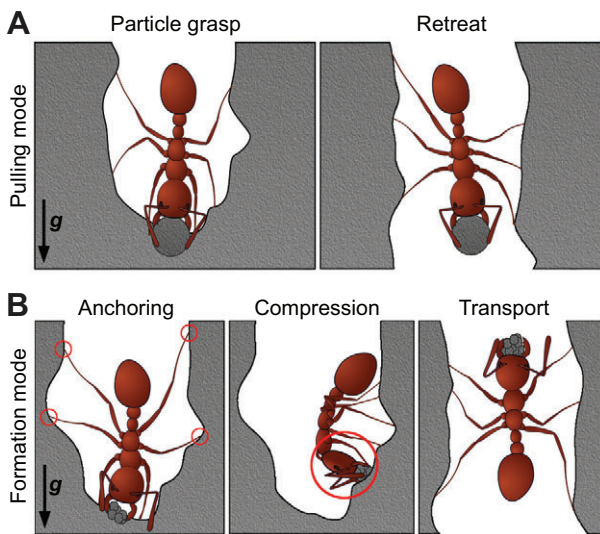


**Fig. 7. Biomechanics of excavation.** Ants exhibited two distinct modes of pellet construction during nest excavation: (A) the pulling mode consisted of an ant grasping the particle at the tunnel face and reversing backwards up the tunnel with the particle in its mandibles; (B) the formation mode consisted of an ant using its forelimbs and antennae to collect and compress particles into a pellet. The pellet is held in the mandibles during transport to the surface.

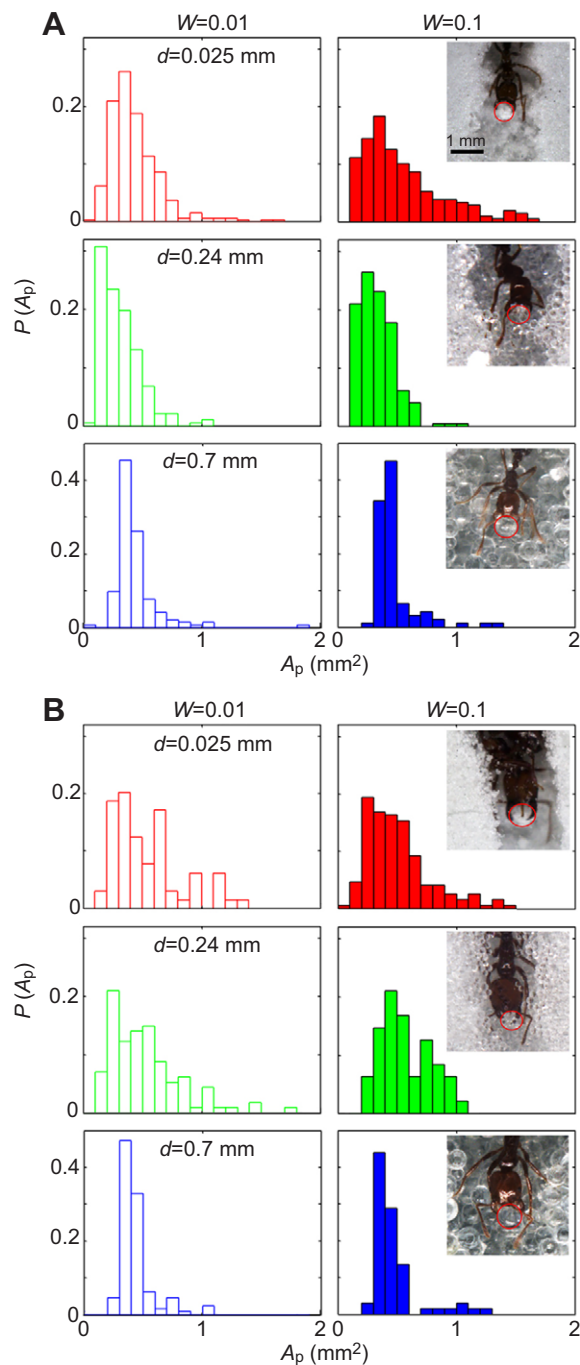


**Fig. 8. Insensitivity of pellet size to substrate and head size.** Probability distributions of pellet area ( $A_p$ ) carried by small ( $h=0.7$  mm; A) and large ( $h=1.2$  mm; B) *S. invicta* workers in substrates of particle size  $d$  and moisture content  $W$ . Images in the insets show snapshots of ants grasping pellets of a moderate size in all  $d$ . Red ellipses enclosing the pellets are drawn as a guide.

### Nest morphology under changing substrate conditions

To our surprise, variation of particle size by nearly a factor of 50 did not result in a large variation in excavated nest volumes provided the water content was sufficiently high ( $W \geq 0.05$ ) (Fig. 2). We expect that such robustness of construction was achieved through the modification of substrate manipulation behavior in response to the changes in the substrate: in smaller particles, ants predominantly used the ‘formation’ mode of pellet formation, while in the larger particles, the ‘pulling’ mode of pellet formation was favored.

Above  $W \approx 0.05$ , nest volume was insensitive to moisture content in all substrates; below this value, nests were small and poorly formed, while above this value, the nests were well formed, featuring deeper tunnels and a more developed network system. These results are in accord with other laboratory studies (Sudd, 1969) and field observations (Ali et al., 1986; Pielström and Roces, 2014) indicating that higher moisture levels of natural soils lead to more sophisticated nest designs in social animals. The increase in nest complexity with substrate moisture could be attributed to the increase in excavation activity of the excavating animals, as observed elsewhere (Sudd, 1969). In addition, increasing substrate moisture leads to increasing substrate cohesiveness.

Despite the wide variation in substrate properties and construction behaviors, we found that substrate yield force was a good predictor of nest depth (Fig. 5C): on average, nest depth increased with increases in substrate cohesiveness, and at higher cohesion levels the majority of experimental colonies reached the bottom of the container. This indicates that high cohesiveness does not prevent ants from excavating pellets but instead allows construction of stronger nests, which are less prone to collapse (Aleksiev et al., 2007). As the stresses acting in the substrate increase with increasing tunnel depth (Muir Wood, 2009), substrate cohesiveness becomes an important factor in tunnel stability. Therefore, nest depth is expected to be sensitive to substrate cohesion. This may explain the observed correlation between these factors. That said, high cohesiveness can still result in digging challenges and perhaps these would manifest in energetics: in cohesive substrates, particles are held together with high attractive forces, which could increase the energetic costs of the excavation (Espinoza and Santamarina, 2010; Toffin et al., 2010; Minter et al., 2013). Future work should address the question of how the energetic cost of tunnel construction is affected by substrate cohesiveness and substrate moisture.

### Active pellet formation for crowded confined transport

We expected that each ant would excavate and transport a larger amount of material as substrate cohesiveness increased, because higher cohesiveness would allow for the formation of more stable pellets (Espinoza and Santamarina, 2010). However, increased cohesiveness did not lead to a substantial increase in pellet size; instead, in all moistures and particle sizes, similarly sized ants formed pellets of similar mean size (see Fig. 8; supplementary material Table S2). About 1/3 of the larger loads decreased in size (by  $\sim 20\%$ ) during transport from tunnel face to exit from field of view (see supplementary material Fig. S3 and Movie 3). This size reduction occurred through passive trimming (or ‘sieving’) when the load-carrying ant interacted with the tunnel walls or other workers. Size reduction also occurred through active pellet reorganization by the ant using mandibles, limbs and antennae. We posit that the creation of intermediate-sized pellets is deliberate, in accord with observations of preference for intermediate size food particles during foraging in *S. invicta* (Hooper-Bùi et al., 2002). This argument is supported by calculations which suggest that neither substrate cohesiveness nor individual ant capabilities limit pellet area  $A_p$  (Materials and methods; supplementary material Table S3); increased substrate cohesion permits the formation of pellets larger than the average pellet size and the largest pellets are well within estimates of the ability of the ants to pull and lift (Materials and methods).

We argue that intermediate-sized pellet selection, through active formation and passive natural sieving, balances the needs of the individual and the collective. For individuals, bulky loads are

undesirable because of their effects on locomotion and sensing: as supplementary material Movie 4 demonstrates, large pellets affect climbing stability and speed (Moll et al., 2013) because of slips and mis-steps. We posit that large pellets also hinder antennal contacts with tunnel walls, which are important for tactile- and chemo-sensing in subterranean environments, as well as for slip and fall recovery (Gravish et al., 2013). The optimal pellet size is also influenced by the needs of the collective. Previously, we discovered that fire ants created tunnels of similar diameter in all substrates (about one body length) (Gravish et al., 2013). We argued that this tunnel size enabled the ants to ascend and descend (without loads) rapidly and stably by offloading control into the environment. Our observations here reveal that this tunnel size limits passing and maneuvering, making it challenging to carry large loads during conditions of tunnel congestion (Dussutour et al., 2004; N.G., G. Gold, A. Zangwill, M.A.D.G. and D.I.G., in review). In such conditions, large loads can also slow or impede tunnel traffic.

### Conclusions

We studied the excavation strategies of fire ants in laboratory substrates modeling substrate conditions encountered in nature. Overall, the incipient nest structure was robust, displaying similar features across a wide range of substrate conditions. However, substrate properties affected the nest construction process and mechanics across multiple scales. At the microscale level of the individual, ants altered their excavation biomechanics and adjusted their activity during excavation as substrate type varied. At the macroscale of the collective, substrate cohesiveness affected nest morphology (in particular, nest depth was correlated with cohesiveness) and, probably, activity of the group. Thus, in accord with their invasive abilities in the wild, in the laboratory, fire ants demonstrated an ability to modify both the biomechanics of substrate manipulation and collective organization of excavation behavior in response to substrate properties.

Like in other studies, the complex nest patterns emerge largely from repeated individual-level interactions. However, these individual behaviors are not ‘simple’ but quite sophisticated. In addition to the biomechanical and control challenges of handling complex materials, we suspect that the ants are controlling their loads to allow for collective motion of the group and the nest properties emerge through decisions that we do not yet understand. We suggest that these patterns of collective behavior are common for the same ant species in different environments. In

support of this, we note that the topological properties of nests in 3D experiments and available data from nest topologies in previous quasi-2D studies (Gravish et al., 2012) were quite similar. The characteristic topological traits were also recently found in termite foraging networks (Lee et al., 2007) and are believed to reflect the demands of the colony to balance food search and transport. This bodes well for future studies of digging behaviors, as 2D studies offer the ability to monitor animals and nests, while our 3D studies are presently restricted to only recording aspects of nest formation.

Further work at the biomechanical as well as the behavioral level is required to better understand such processes in ants, as well as how such features may be generalized among other social excavators. That said, as excavation cannot be considered apart from physical properties of the substrates and constraints of underground construction, we expect that some of the principles discovered should hold in other ant species and perhaps other social diggers.

### MATERIALS AND METHODS

#### Ants

Twenty *S. invicta* nests were collected during the spring, summer and autumn of 2012 and 2013 at the Research and Education Garden of the University of Georgia, GA, USA, and the Chattahoochee-Oconee National Forest, GA, USA. Nest collection and colony extraction were performed according to methods found in Jouvenaz et al. (1977). Ants were housed in plastic bins for 2–3 months at an ambient room temperature of  $23\pm 3^\circ\text{C}$  with a relative humidity of  $30\pm 2\%$ , and fed *Vespula* larvae and supplied with tap water twice a week.

#### Digging arena

A sieving technique was developed to ensure repeatable and uniform moisture content and distribution (and compaction) of the prepared laboratory substrate. The sieving apparatus consisted of two square containers ( $30.5\times 30.5\text{ cm}^2$ ) mounted on a vibrating table (Fig. 9A). The base of the top container was a wire mesh with  $3\times 3\text{ mm}^2$  spacing (Sharpe, 2013; Sharpe et al., 2015). A desired weight of water was added to the simulated substrate (acquired from Jaygo Inc., Potters Industries Inc.) and thoroughly mixed. Wet substrate was loaded into the top container. The bottom container had an insert which housed hollow aluminium cylinders (inner diameter 3.5 cm, height 14.5 cm). Upon sinusoidal vertical vibration (frequency 60 Hz, amplitude 1.75 mm), substrate passed through the mesh into the bottom container, filling the cylinders. Depending on moisture and particle size, the time to fill the tubes with substrate completely was between 5 and 20 min. To achieve consistent compaction (volume fraction  $0.6\pm 0.025$ ), tubes were shaken for an additional 10 min. Excess material

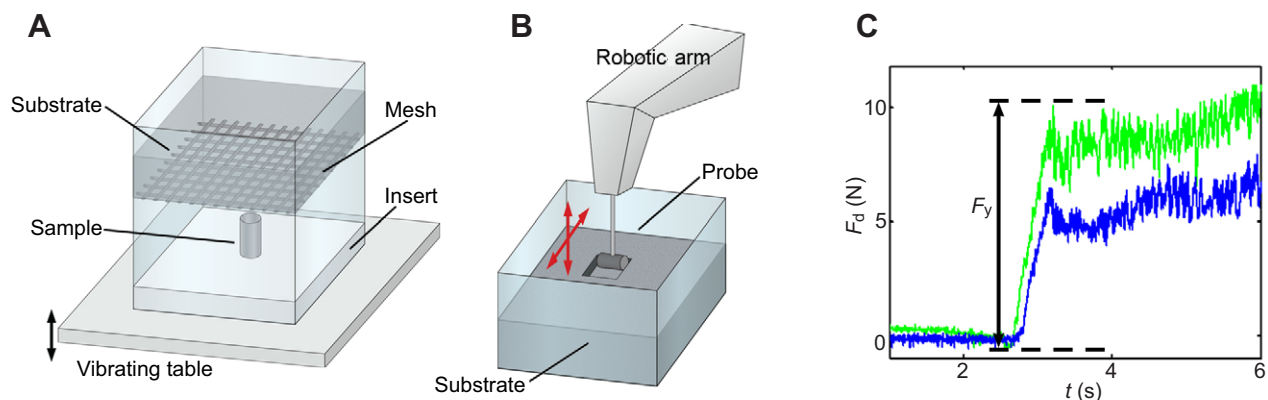


**Fig. 9. Techniques for substrate preparation and analysis.** (A) Sieving apparatus. (B) Schematic diagram of the drag experiment. (C) Example of force–time curves in  $W=0.01$  (blue, bottom curve) and  $W=0.15$  (green, top curve) wet substrates. Yield force,  $F_y$ , is indicated by the arrow.  $F_d$ , drag force.



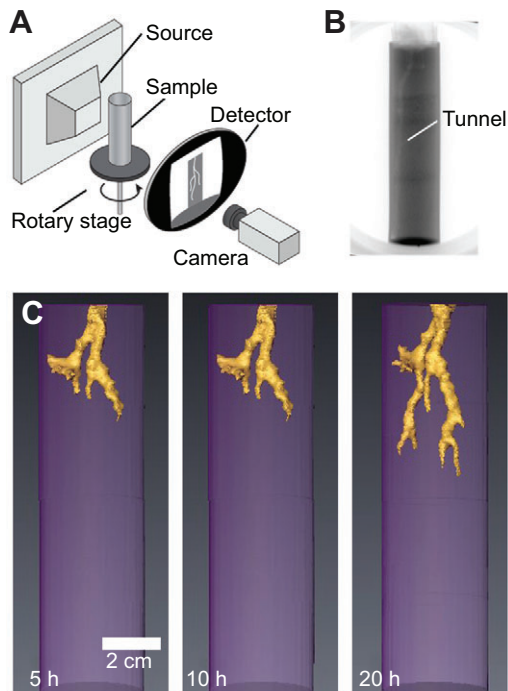


**Fig. 10. X-ray system for nest visualization.** (A) Schematic diagram of the X-ray CT system. (B) Single X-ray projection of the sample. (C) Reconstructions of growing tunnels after 5, 10 and 20 h.

was removed and the containers with substrate were connected to an enclosure housing  $100 \pm 10$  fire ants. The floor of the enclosure had a single entry point,  $\sim 0.5$  cm in diameter, forcing the ants to begin excavation away from the container walls. After 20 h, a sample of substrate was taken from every container and the moisture content of the substrate was determined by drying the sample. Because the containers were sealed during the experiment, the measured change of the moisture content was not significant.

To characterize substrate cohesive properties, the insert was removed from the container and the substrate was sieved directly into the bottom container until it reached 7 cm in height under the conditions described above. Excess substrate was removed with an aluminium slider, leaving the surface flat. Summarizing, this technique allowed the creation of substrate states of different gravimetric moisture content  $W$  (defined as the ratio of total water weight to total solid weight) in the range of 0.01 to 0.2.

### Cohesion and force measurements

The macroscopic cohesive properties of the substrate were measured by insertion and drag of a small stainless steel cylinder (diameter 1.6 cm and length 3.81 cm) in the substrate (Fig. 9B; Li et al., 2013; Sharpe et al., 2015). The cylinder was attached via a support rod (diameter 0.63 cm) to a force–torque sensor (ATI Industrial, USA) mounted on a robotic arm (CRS Robotics, Canada). The rod was attached such that its long axis was normal to the supporting rod and the drag direction. In each experiment, the rod was pushed 3.2 cm deep in the substrate (as measured from its long axis) and after a 2 s pause it was dragged 12.7 cm through the substrate. The drag speed was set to  $1 \text{ cm s}^{-1}$ . For simplicity, the first peak of the drag force,  $F_d$  (material yield point denoted  $F_y$ ) (Fig. 9C), was used as a measure of substrate cohesiveness.

### X-ray imaging

A custom-made X-ray CT system was used to study the time evolution and structure of 3D networks of tunnels excavated in 20 h long experiments (Fig. 10). The aluminium cylinder with ants was mounted on the rotary stage (Lin Engineering, Morgan Hill, CA, USA) and 400 projections of excavated networks were acquired per rotation using a cone-beam CT X-ray system

(Philips, USA; 110 kVp, 3 mA) and a high-speed camera (Phantom v210, Vision Research Inc., USA).

The tunnel cross-sections were reconstructed using an open source reconstruction tool (OSCaR, Nargol Rezvani) based on the Feldkamp–Davis–Kress algorithm, and visualized and analyzed with Avizo 8.0 software (FEI Visualization Sciences Group). The software was used to measure  $D$  and  $V$  and to extract morphological and topological properties of the nest networks. Visualization of reference shapes of known volume revealed that volume measurements were accurate to within 5%. X-ray CT scans were performed to characterize nest morphology after 5, 10 and 20 h of excavation. Nine experiments were performed at each substrate particle size–substrate moisture combination. JMP software (SAS Institute Inc., USA) was used for statistical analysis.

### Imaging ant activity in quasi 2D setups

Groups of 15 large and 15 small workers (with head width  $h=1.2$  and  $0.7$  mm, respectively) were isolated in a transparent plastic cylindrical container filled with wet granular media. The ants were sampled from nine *S. invicta* colonies; at least three groups of ants from three different colonies were subjected to each experimental condition. In the digging arena, the ants were placed on top of a thin plastic insert to separate them from the substrate. An entry hole corresponding to the ant tunnel's natural diameter (5 mm)

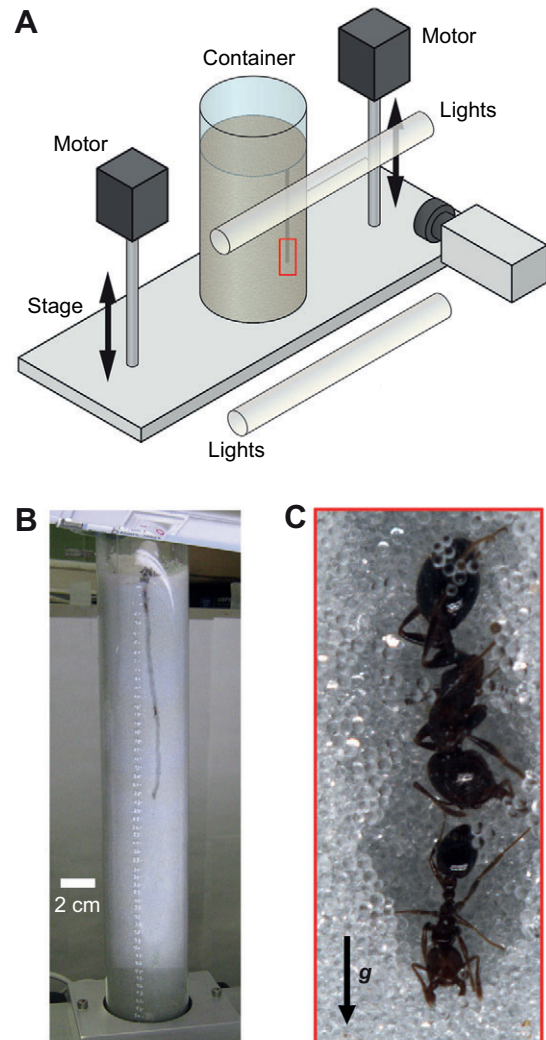


**Fig. 11. Laboratory experiments to visualize substrate excavation by fire ants in crowded tunnels.** (A) Schematic diagram of the experimental setup. (B) Digital image of the digging arena. (C) Camera snapshot: large and small ants excavating a tunnel. The arrow shows the direction of gravity ( $g$ ).

(Markin et al., 1973; Markin et al., 1975; Cassill et al., 2002) was placed on the edge of the plastic insert to direct the ants' excavation near the transparent wall of the digging arena (Fig. 11B,C). A 0.5 cm deep precursor indentation was created to facilitate tunnel construction. The ants did not branch the tunnel within the time of the experiment.

To track ant behaviors and excavation progression over time, the digging arena was mounted on a motorized stage (Fig. 11A) operated by two linear actuators (Firgelli Technologies, Canada), controlled through LabView-based software. Image sequences (~30 s duration) were recorded at 50 frames  $s^{-1}$  with 5 s intervals between the image sequences over 10 h by a camera (Point Grey Research, Canada) focused on the tunnel excavation face. The position of the container was adjusted automatically so that ~1.5 cm of tunnel above the excavation face was always visible. These image sequences were analyzed to establish specific excavation strategies for different  $W$  and  $d$ . JMP software was used for statistical analysis, as described above.

### Differences in 2D and 3D nests

There were differences between 3D and 2D nests; in particular, the CT reconstructions revealed a structural feature of nest networks that is observed in natural nests (Tschinkel, 2006) but that we did not observe in our previous experiments in quasi 2-D containers. In seven out of 189 trials, the ants built barrel-like 3D chambers (see supplementary material Fig. S1), 3–5 times wider than typical network tunnels. These chambers occurred in all tested substrates and appeared within the first 30% (~2.5 cm to the substrate surface) of the tunnel length and comprised  $30 \pm 10\%$  of the total network volume. The chambers were constructed by widening the tunnel intersection near the high degree node.

### Pellet size estimates

The agglomerate size was defined as the area,  $A_p$ , of an ellipse that completely enclosed the largest projection of the load (supplementary material Fig. S2A). Measurements reported were obtained as ants exited the field of view (3–4 body lengths away from the tunnel face), as the pellet size was adjusted upon transport. Supplementary material Fig. S2B shows an example of the distribution of pellet sizes created by fire ants in a single experiment.

In clay and fine substrates ( $d=0.025$  and  $0.24$  mm), the mass of the pellet was estimated as  $m=\rho V_p C(1+W)$ , where  $\rho=2.5$  g  $cm^{-3}$  is the density of soda lime glass,  $V_p$  is the mean pellet volume,  $C=0.66$  is the assumed substrate compaction, and  $W=0.1$  is the substrate moisture. The pellet volume was calculated as the volume of an ellipsoid  $V_p = \frac{4}{3} \bar{A}_p \sqrt{\bar{A}_p} / \pi$ , where  $\bar{A}_p$  is a mean pellet area for a given  $d$  and  $W$  (supplementary material Table S3). In coarse substrates ( $d=0.7$  mm), where the ants most frequently excavated and transported one particle at a time, pellet mass was defined as the mass of the average particle.

### Ant strength estimates

As noted in Sudd (1965) for *Myrmica rubra* L. and *Formica lugubris* Zett., ants are capable of producing pulling forces 30–40 times their own weight. The average mass of an *S. invicta* worker is 3.2 mg (Tschinkel, 2006) and the corresponding pulling force is about 1256  $\mu N$  (supplementary material Table S3). An estimate of the capillary attraction force acting between two spherical particles in contact is given by  $F \approx 2\pi R\sigma$  (Herminghaus, 2005), where  $R$  is the particle radius and  $\sigma=0.072$  N  $m^{-1}$  is the water surface tension. The calculated capillary forces in the substrate are expected to be lower than the pulling force (including mandible grasp strength and musculature pulling force) produced by the ant (supplementary material Table S3). The lifting ability of the animal is also unlikely to be a limiting factor contributing to the observed prevalence of mean-sized pellets during excavation. The observed masses of the mean-sized pellets were  $m=0.47$  mg (clay-like substrate),  $m=0.37$  mg (fine substrate) in fine particles and  $m=0.45$  mg (coarse substrate), several times less than the average mass (~2 mg; Markin et al., 1973) of one *S. invicta* worker. Fire ants are capable of lifting and carrying objects at least 3–4 times heavier than their own mass (Sudd, 1965; Tschinkel, 2006), indicating that the mass of the average

observed pellet size is well below the animals' maximum strength limitations (supplementary material Table S3).

Furthermore, the weight of a single particle in the pellet is much smaller than the magnitude of the capillary cohesion forces (supplementary material Table S3). In fact, as we occasionally observed pellets with an area significantly larger than the mean pellet size area in all substrates (supplementary material Fig. S2, Table S2), capillary cohesion should not be the main factor constraining pellet size.

### Effect of tunnel size on pellet size

An additional experiment was conducted to study the effect of tunnel size on pellet sizes created by worker ants. In this experiment, 30 ants were introduced to the clay-like substrate ( $d=0.025$  mm) at  $W=0.1$  where the diameter of the initial indent was doubled using a rod penetrating into the substrate (to  $d=1$  cm). In response to the larger indentation, most of the ants immediately relocated below the substrate surface, crowding around the excavation face and commencing excavation of a tunnel of the normal diameter ( $d \leq 5$  mm). Within the first 2–3 h of the experiment, tunnel construction continued in the crowded conditions, after which the size of the tunnel was adjusted to the size observed in all other experiments. As a result, the average size of the pellets carried by the ants 3–4 body lengths away from the tunnel face was equal to  $\bar{A}_p$  ( $d=0.025$  mm) of  $0.43 \pm 0.03$  mm<sup>2</sup> and was not affected (one-way ANOVA,  $F_{1,400}=0.48$ ,  $P=0.48$ ) by the size of the incipient tunnel (supplementary material Fig. S3).

### Acknowledgements

The authors would like to acknowledge Anthony Stranko and Romik Srivastava for help with animal care, experimental work and data analysis.

### Competing interests

The authors declare no competing or financial interests.

### Author contributions

D.M. participated in the development, design and execution of the experiments, in data collection and analysis, and in manuscript writing. N.G. participated in the development and design of the experiments and in manuscript writing. G.R. and R.K. participated in the execution of experiments, data collection and animal care. M.A.D.G. and D.I.G. participated in the development and design of the experiments, and supervised data analysis and manuscript writing.

### Funding

This work was supported by NSF PoLS grants 0957659 and 1205878.

### Supplementary material

Supplementary material available online at <http://jeb.biologists.org/lookup/suppl/doi:10.1242/jeb.113795/-/DC1>

### References

- Aleksiev, A. S., Sendova-Franks, A. B. and Franks, N. R. (2007). The selection of building material for wall construction by ants. *Anim. Behav.* **73**, 779–788.
- Ali, A. D., Hudnall, W. H. and Reagan, T. E. (1986). Effects of soil types and cultural practices on the fire ant, *Solenopsis invicta*, in sugarcane. *Agriculture Ecosyst. Environ.* **18**, 63–71.
- Bardunias, P. M. and Su, N.-Y. (2010). Queue size determines the width of tunnels in the formosan subterranean termite (Isoptera: Rhinotermitidae). *J. Insect Behav.* **23**, 189–204.
- Buhl, J., Gautrais, J., Deneubourg, J.-L. and Theraulaz, G. (2004a). Nest excavation in ants: group size effects on the size and structure of tunneling networks. *Naturwissenschaften* **91**, 602–606.
- Buhl, J., Gautrais, J., Sole, R. V., Kuntz, P., Valverde, S., Deneubourg, J. L. and Theraulaz, G. (2004b). Efficiency and robustness in ant networks of galleries. *Eur. Phys. J. B* **42**, 123–129.
- Burd, M. (2000). Body size effects on locomotion and load carriage in the highly polymorphic leaf-cutting ants *Atta colombica* and *Atta cephalotes*. *Behav. Ecol.* **11**, 125–131.
- Campbell, D. J., Stafford, J. V. and Blackwell, P. S. (1980). The plastic limit, as determined by the drop-cone test, in relation to the mechanical behaviour of soil. *J. Soil Sci.* **31**, 11–24.
- Cassill, D., Tschinkel, W. R. and Vinson, S. B. (2002). Nest complexity, group size and brood rearing in the fire ant, *Solenopsis invicta*. *Insectes Soc.* **49**, 158–163.

- Coleman, D. C., Crossley, D. A. and Hendrix, P. F. (2004). *Fundamentals of Soil Ecology*. Amsterdam; Boston: Elsevier Academic Press.
- Decaëns, T., Jiménez, J. J., Gioia, C., Measey, G. J. and Lavelle, P. (2006). The values of soil animals for conservation biology. *Eur. J. Soil Biol.* **42**, S23-S38.
- Dussutour, A., Fourcassié, V., Helbing, D. and Deneubourg, J.-L. (2004). Optimal traffic organization in ants under crowded conditions. *Nature* **428**, 70-73.
- Espinoza, D. N. and Santamarina, J. C. (2010). Ant tunneling—a granular media perspective. *Granular Matter* **12**, 607-616.
- Evans, H. E. (1966). The behavior patterns of solitary wasps. *Annu. Rev. Entomol.* **11**, 123-154.
- Farji-Brener, A. G. (2003). Microhabitat selection by antlion larvae, *Myrmeleon crudelis*: effect of soil particle size on pit-trap design and prey capture. *J. Insect Behav.* **16**, 783-796.
- Gravish, N., Garcia, M., Mazouchova, N., Levy, L., Umbanhowar, P. B., Goodisman, M. A. D. and Goldman, D. I. (2012). Effects of worker size on the dynamics of fire ant tunnel construction. *J. R. Soc. Interface* **9**, 3312-3322.
- Gravish, N., Monaenkova, D., Goodisman, M. A. D. and Goldman, D. I. (2013). Climbing, falling, and jamming during ant locomotion in confined environments. *Proc. Natl. Acad. Sci. USA* **110**, 9746-9751.
- Herminghaus, S. (2005). Dynamics of wet granular matter. *Advances in Physics* **54**, 221-261.
- Hölldobler, B. and Wilson, E. O. (2009). *The Superorganism: The Beauty, Elegance, and Strangeness of Insect Societies*. New York: W. W. Norton.
- Hooper-Bùi, L. M., Appel, A. G. and Rust, M. K. (2002). Preference of food particle size among several urban ant species. *J. Econ. Entomol.* **95**, 1222-1228.
- Huang, M. H. (2010). Multi-phase defense by the big-headed ant, *Pheidole obtusospinosa*, against raiding army ants. *J. Insect Sci.* **10**.
- Jouvenaz, D. P., Allen, G. E., Banks, W. A. and Wojcik, D. P. (1977). A survey for pathogens of fire ants, *Solenopsis* spp., in the Southeastern United States. *Fla. Entomol.* **60**, 275-279.
- Kadochova, S. and Frouz, J. (2013). Thermoregulation strategies in ants in comparison to other social insects, with a focus on red wood ants (*Formica rufagroup*). *F1000Research* **2**, 280.
- Korb, J. (2003). Thermoregulation and ventilation of termite mounds. *Naturwissenschaften* **90**, 212-219.
- Lee, S.-H., Bardunias, P. and Su, N.-Y. (2007). Optimal length distribution of termite tunnel branches for efficient food search and resource transportation. *Biosystems* **90**, 802-807.
- Li, C., Zhang, T. and Goldman, D. I. (2013). A terradynamics of legged locomotion on granular media. *Science* **339**, 1408-1412.
- Markin, G. P., Dillier, J. H. and Collins, H. L. (1973). Growth and development of colonies of the red imported fire ant, *Solenopsis invicta*. *Ann. Entomol. Soc. Am.* **66**, 803-808.
- Markin, G. P., O'Neal, J. and Dillier, J. (1975). Foraging tunnels of the red imported fire ant, *Solenopsis invicta* (Hymenoptera: Formicidae). *J. Kans. Entomol. Soc.* **48**, 83-89.
- Mason, G. L. (1958). Food habits, baits, and attractants concerning the imported fire ant, *Solenopsis saevissima* var. *richteri* Forel. MS thesis, Mississippi State University.
- Minter, N. J., Sendova-Franks, A. B. and Franks, N. R. (2013). Nest-seeking rock ants (*Temnothorax albipennis*) trade off sediment packing density and structural integrity for ease of cavity excavation. *Behav. Ecol. Sociobiol.* **67**, 1745-1756.
- Mitarai, N. and Nori, F. (2006). Wet granular materials. *Adv. Phys.* **55**, 1-45.
- Moll, K., Roces, F. and Federle, W. (2013). How load-carrying ants avoid falling over: mechanical stability during foraging in *Atta vollenweideri* grass-cutting ants. *PLoS ONE* **8**, e52816.
- Muir Wood, D. (2009). *Soil Mechanics: A One-Dimensional Introduction*. Cambridge: Cambridge University Press.
- Muma, M. H. (1967). Basic behavior of North American Solpugida. *Fla. Entomol.* **50**, 115.
- Nowak, S., Samadani, A. and Kudrolli, A. (2005). Maximum angle of stability of a wet granular pile. *Nat. Phys.* **1**, 50-52.
- Oi, D. H., Williams, D. F., Pereira, R. M., Horton, P. M., Davis, T. S., Hyder, A. H., Bolton, H. T., Zeichner, B. C., Porter, S. D. and Hoch, L. A. (2008). Combining biological and chemical controls for the management of red imported fire ants (Hymenoptera: Formicidae). *Am. Entomol.* **54**, 46-55.
- Perna, A., Jost, C., Couturier, E., Valverde, S., Douady, S. and Theraulaz, G. (2008). The structure of gallery networks in the nests of termite *Cubitermes* spp. revealed by X-ray tomography. *Naturwissenschaften* **95**, 877-884.
- Pielström, S. and Roces, F. (2014). Soil moisture and excavation behaviour in the chaco leaf-cutting ant (*Atta vollenweideri*): digging performance and prevention of water inflow into the nest. *PLoS ONE* **9**, e95658.
- Price, D. L. and May, M. (2009). Behavioral ecology of *Phanaeus* dung beetles (Coleoptera: Scarabaeidae): review and new observations. *Acta Zool. Mex.* **25**, 211-238.
- Ratcliffe, B. C. and Fagerstrom, J. A. (1980). Invertebrate lebensspuren of holocene floodplains - their morphology, origin and paleoecological significance. *J. Paleontol.* **54**, 614-630.
- Rhoades, W. C. and Davis, D. R. (1967). Effects of meteorological factors on the biology and control of the imported fire ant. *J. Econ. Entomol.* **60**, 554-558.
- Rutin, J. (1996). The burrowing activity of scorpions (*Scorpio maurus palmatus*) and their potential contribution to the erosion of Hamra soils in Karkur, central Israel. *Geomorphology* **15**, 159-168.
- Sakagami, S. F. and Hayashida, K. (1962). Work efficiency in heterospecific ant groups composed of hosts and their labour parasites. *Anim. Behav.* **10**, 96-104.
- Sharpe, S. S. (2013). Control of burial and subsurface locomotion in particulate substrates. PhD thesis, Department of Biomedical Engineering, Georgia Institute of Technology, pp. 238.
- Sharpe, S. S., Koehler, S. A., Kuckuk, R., Serrano, M., Vela, P. and Goldman, D. I. (2015). Locomotor benefits of being a slender and slick sand swimmer. *J. Exp. Biol.* **218**, 440-450.
- Sprague, J. C. (2013). *Costs and Benefits of an Extended Phenotype: Chambers Made by Manduca sexta Larvae*. Missoula, MT: The University of Montana.
- Springthorpe, D., Gravish, N., Mazouchova, N., Goldman, D. I. and Full, R. J. (2013). Burrowing biomechanics of the ghost crab. *Integr. Comp. Biol.* **53**, E206-E206.
- Strauch, S. and Herminghaus, S. (2012). Wet granular matter: a truly complex fluid. *Soft Matter* **8**, 8271-8280.
- Sudd, J. H. (1965). The transport of prey by ants. *Behaviour* **25**, 234-271.
- Sudd, J. H. (1969). The excavation of soil by ants. *Z. Tierps.* **26**, 257-276.
- Sudd, J. H. (1972). The absence of social enhancement of digging in pairs of ants (*Formica lemani* Bondroit). *Anim. Behav.* **20**, 813-819.
- Taber, S. W. (2000). *Fire Ants*. College Station, TX: Texas A & M University Press.
- Toffin, E., Kindekens, J. and Deneubourg, J.-L. (2010). Excavated substrate modulates growth instability during nest building in ants. *Proc. R. Soc. B Biol. Sci.* **277**, 2617-2625.
- Tschinkel, W. R. (2006). *The Fire Ants*. Cambridge, MA: Belknap Press of Harvard University Press.
- Villani, M. G., Allee, L. L., Díaz, A. and Robbins, P. S. (1999). Adaptive strategies of edaphic arthropods. *Annu. Rev. Entomol.* **44**, 233-256.
- Whitford, W. G. and Ettershank, G. (1975). Factors affecting foraging activity in chihuahuan desert harvester ants. *Environ. Entomol.* **4**, 689-696.

**Table S1.** The effect of substrate particle size ( $d$ ) and moisture ( $W$ ) on the mean tunnel depth ( $\bar{D} \pm s.d.$ ) and mean tunnel volume ( $\bar{V} \pm s.d.$ ).

$W$	$d, mm$	$\bar{D} \pm s.d., cm$	$\bar{V} \pm s.d., cm^3$
0.01	0.025	$3.2 \pm 0.9$	$0.5 \pm 0.3$
0.03	0.025	$3.6 \pm 3.5$	$0.6 \pm 0.4$
0.05	0.025	$6.9 \pm 5$	$1.1 \pm 0.3$
0.1	0.025	$9 \pm 3.9$	$1.6 \pm 0.6$
0.15	0.025	$9.4 \pm 3.9$	$1.4 \pm 0.7$
0.18	0.025	$9.9 \pm 2.5$	$1.8 \pm 1$
0.2	0.025	$7.8 \pm 2.5$	$1.4 \pm 0.5$

$W$	$d, mm$	$\bar{D} \pm s.d., cm$	$\bar{V} \pm s.d., cm^3$
0.01	0.24	$4.4 \pm 2.4$	$0.4 \pm 0.3$
0.03	0.24	$8.1 \pm 3.6$	$0.9 \pm 0.7$
0.05	0.24	$11.6 \pm 1.8$	$1.9 \pm 0.6$
0.1	0.24	$10.1 \pm 3.1$	$1.3 \pm 0.8$
0.15	0.24	$12.5 \pm 1.5$	$1.9 \pm 0.7$
0.18	0.24	$9.3 \pm 2.5$	$1 \pm 0.7$
0.2	0.24	$12.2 \pm 1.7$	$1.7 \pm 0.9$

$W$	$d, mm$	$\bar{D} \pm s.d., cm$	$\bar{V} \pm s.d., cm^3$
0.01	0.7	$5.1 \pm 4.2$	$1.1 \pm 0.5$
0.03	0.7	$7.2 \pm 4.2$	$1.1 \pm 0.7$
0.05	0.7	$7.4 \pm 4.9$	$1.3 \pm 1$
0.1	0.7	$9.6 \pm 3$	$1.5 \pm 0.6$
0.15	0.7	$8.4 \pm 2.9$	$1.4 \pm 0.5$
0.18	0.7	$5.8 \pm 3.7$	$1.3 \pm 0.7$
0.2	0.7	$4.3 \pm 3.1$	$1.1 \pm 0.5$

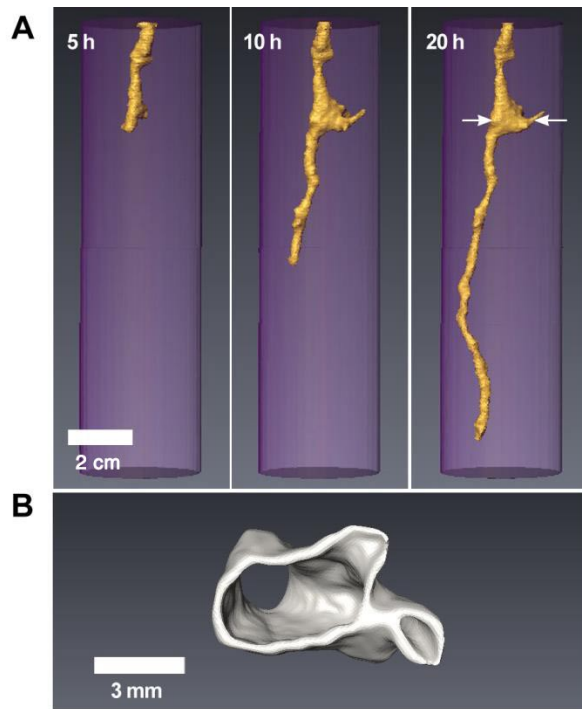


**Fig. S1. Example of 3D chambers.** A) Time lapse of construction of the tunnel with 3D chamber. Arrows show the height at which the chamber cross-section B) was taken.

**Table S2.** The effect of substrate particle size ( $d$ ) and moisture ( $W$ ) on the mean pellet size ( $\bar{A}_p \pm \text{s.d.}$ ) and maximum pellet size ( $A_{max}$ ) created by small and large ants of head-size ( $h$ ).

$d$ (mm)	$W$	$h$ (mm)	$\bar{A}_p \pm \text{s.d.}$ (mm <sup>2</sup> )	$A_{max} \pm \text{s.d.}$ (mm <sup>2</sup> )
0.025	0.01	0.7	$0.38 \pm 0.21$	1.65
		1.2	$0.49 \pm 0.29$	1.32
	0.1	0.7	$0.49 \pm 0.34$	1.66
		1.2	$0.49 \pm 0.35$	2.86
0.24	0.01	0.7	$0.27 \pm 0.17$	1.1
		1.2	$0.48 \pm 0.31$	1.74
	0.1	0.7	$0.28 \pm 0.15$	1
		1.2	$0.56 \pm 0.3$	1.64
0.7	0.01	0.7	$0.38 \pm 0.19$	1.85
		1.2	$0.38 \pm 0.15$	1.1
	0.1	0.7	$0.42 \pm 0.18$	1.32
		1.2	$0.42 \pm 0.21$	1.21

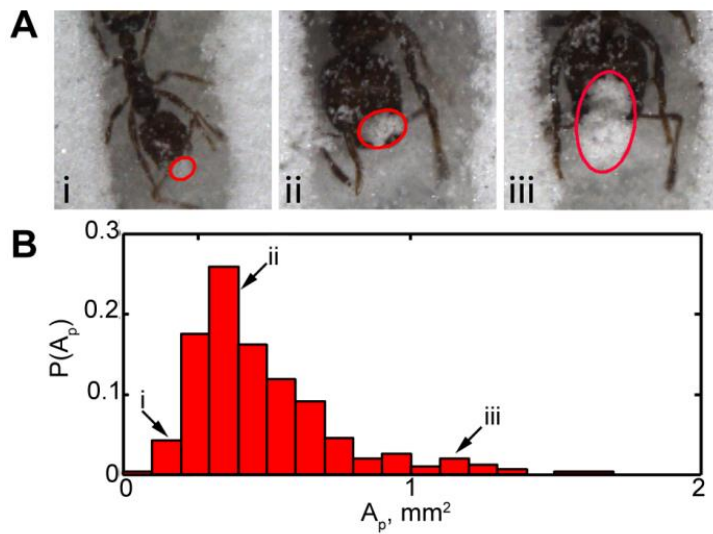


**Fig. S2. Distribution of pellet sizes excavated in experiment.** A) Examples of pellets created by *S. invicta* in  $d = 0.025$  mm substrate, B). Labels i,ii,iii show snapshots of ants carrying representative pellets from the indicated points in the distribution B). The red ellipses enclose the pellet and are drawn to guide the eye.

**Table S3.** Estimates of capillary forces, ant strength and particle weight.

$d$ (mm)	Capillary force ( $\mu\text{N}$ )	Single particle weight ( $\mu\text{N}$ )
0.025	5.65	0.0002
0.24	54.26	0.18
0.7	158.26	4.4
Ant pulling force ( $\mu\text{N}$ )	1256	

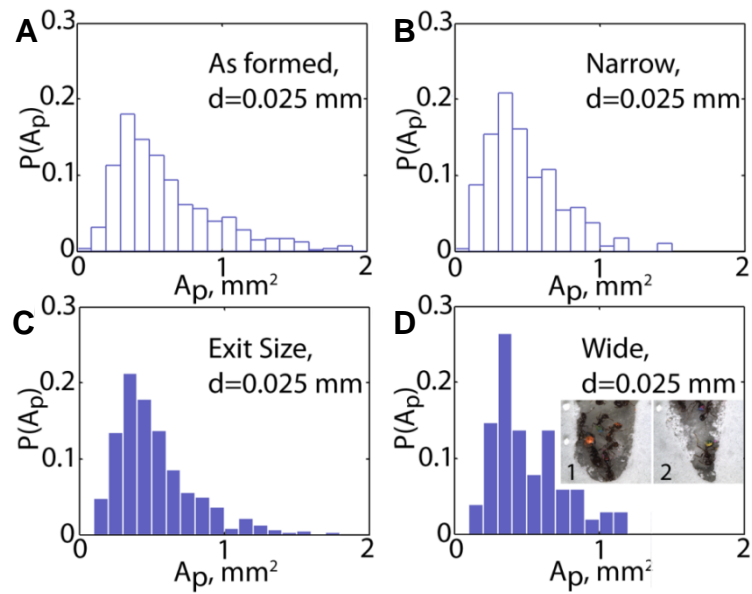
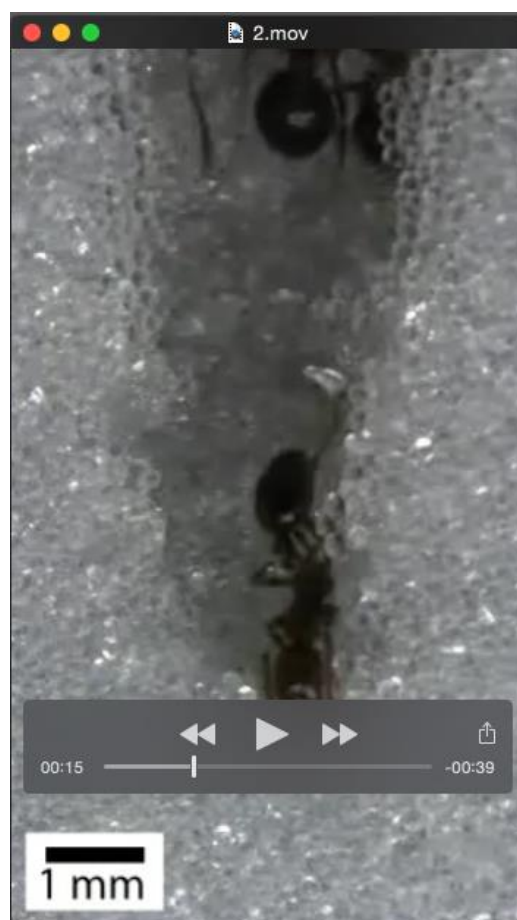


**Fig. S3.** Pellet size distribution in  $d = 0.025$  mm substrate directly after pellet formation (A) and 3-4 B.L. away from the tunnel face (referred to as 'Exit size') (C). Probability distribution of pellet area carried by *S. invicta* in case of narrow (B) ( $\leq 0.5$  cm) and wide ( $\sim 1$  cm) (d) incipient tunnels in 0.025 mm substrate,  $W = 0.1$ . Insert: Tunnel narrowing by ants with time.



**Movie 1.** “Pulling mode”: Typical excavation behavior of *S. invicta* worker (recorded at 50 fps, playing at 30 fps).





**Movie 2.** “Formation mode”: Typical excavation behavior of *S. invicta* worker (recorded at 50 fps, playing at 20 fps).



**Movie 3.** Example of pellet breakage due to the ants contact in the tunnel (recorded at 50 fps, playing at 30 fps).



**Movie 4.** Unsteady locomotion of the *S. invicta* worker, carrying relatively large pellet (recorded at 50 fps, playing at 15 fps).